Building and Environment 78 (2014) 199–211

Contents lists available at ScienceDirect

Building and Environment

journal homepage: www.elsevier.com/locate/buildenv

Effects of plant and substrate selection on thermal performance of green roofs during the summer

Mingjie Zhao [a,*], Paulo Cesar Tabares-Velasco [b], Jelena Srebric [c,**], Sridhar Komarneni [d], Robert Berghage [e]

[a] Department of Architectural Engineering, The Pennsylvania State University, University Park, PA 16802, USA
[b] National Renewable Energy Laboratory, Golden, CO 80401, USA
[c] Department of Mechanical Engineering, University of Maryland, College Park, MD 20742, USA
[d] Materials Research Institute, The Pennsylvania State University, University Park, PA 16802, USA
[e] Department of Horticulture, The Pennsylvania State University, University Park, PA 16802, USA

ARTICLE INFO

Article history:
Received 5 October 2013
Received in revised form
18 February 2014
Accepted 22 February 2014
Available online 12 March 2014

Keywords:
Green roof performance
Plant and substrate selection
Green roof model
Heat flux
Net radiation

ABSTRACT

Green roof assemblies influence the total roof surface energy balance for a building. The energy balance for a green roof depends mostly on the selection of plants and substrates suitable for the building's location. This study measured thermal properties of common green roof materials and selected two types of plants and substrates to simulate transient thermal performance of different green roof assemblies. The selected plants and substrates have the highest and lowest reflectivity values to establish upper and lower bounds of thermal performance. The simulations use a previously developed green roof model including weather data for four cities representing different climate zones in the U.S. Based on the simulations, substrate heat fluxes and net radiation fluxes are compared for five days in July of the typical meteorological year. The results show that green roof assemblies receive net radiation fluxes that differ by 20%, and peak net radiation fluxes that differ by 16%, due to their different spectral reflectivity values. However, the substrate heat fluxes are similar for different green roof assemblies, as a roof insulation layer diminished this flux. Overall, the material selection of green roof assemblies is more important for buildings located in climate zone 4 or 5 than buildings located in climate zone 2 or 3, where limited water availability for evapotranspiration during hot, dry summers results in little thermal performance variability. Independent of the climate zones, simulation results show that the plant type has an important effect on the net radiation.

1. Introduction

Green roofs have been gaining popularity as a sustainable building technology with a range of benefits. Many buildings use green roofs to store rainwater and then gradually release it as a means of storm water management. Green roofs with appropriate plants can efficiently reduce runoff while providing natural filtration, and do not require watering [1]. Furthermore, by providing additional shading, evapotranspiration, and insulation compared to traditional reflective roof coverings, green roofs play an important role in the total roof surface energy balance used in building energy simulations. Green roofs can reduce the urban heat island effect, protect the building envelop from exposure to excessive daily temperature swings, and decrease cooling and heating requirements [2–4]. Finally, green roofs have life cycle benefits as they can last longer than conventional roofs with lower maintenance costs [5–7].

A typical green roof consists of three layers (from bottom to top): a drainage layer, a substrate layer (growing medium), and a plant layer. The substrate layer typically includes three main components: a lightweight inorganic aggregate, compost, and sand [6]. A green roof designer has many choices for substrates and plants based on local climate, material prices and aesthetic requirements. The substrate material's thermal properties, such as thermal conductivity [7] and specific heat capacity [6,8], can significantly vary between green roof components, causing varying influences on the green roof energy balance. In addition, substrate

* Corresponding author. Tel.: +1 814 321 7538; fax: +1 814 863 4789.
** Corresponding author. Tel.: +1 301 405 7276.
E-mail addresses: mxz190@psu.edu, zhaomj1@gmail.com (M. Zhao), paulo.tabares@nrel.gov (P.C. Tabares-Velasco), jsrebric@umd.edu (J. Srebric), sxk7@psu.ed (S. Komarneni), rdberghage@mac.com (R. Berghage).

http://dx.doi.org/10.1016/j.buildenv.2014.02.011
0360-1323/

Nomenclature

C volumetric specific heat, mJ/(m^3 K)
C_p specific heat, mJ/(kg K)
ρ density, kg/m^3
K thermal conductivity, W/m K
$R_{sh,abs,plants}$ absorbed short wave or solar radiation by the plants
$R_{sh,abs,substrate}$ absorbed solar radiation by substrate underneath the plants
$Q_{IR,plants,sky}$ radiative heat transfer between plants and sky (W/m^2)
$Q_{IR,,subs,cov,sky}$ thermal radiation or radiative heat exchange between substrate and sky, W/m^2
$Q_{film,plants}$ heat transfer between plants and the surrounding environment (W/m^2)
Q_{IR} long wave radiation between the plant and the top substrate layer (W/m^2)
$Q_{S,P}$ convective heat transfer between the top substrate layer and the surrounding air (W/m^2)
$Q_{substrate}$ conductive heat fluxes through green roof substrate (W/m^2)
$Q_{IR,sky}$ long wave radiation exchanged between substrate and sky (W/m^2)
$\tau_{plants,IR}$ long-wave transmittance of a canopy, 0.1256
ε_{plants}, $\varepsilon_{substrates}$ emissivity of plant and substrates
T_{plants}, T_{sky}, $T_{top,substrate}$, $T_{air,ref}$, T_{soil} plants' average temperature, sky temperature, temperature of top layer of substrate, air temperature, substrate temperature, K
σ Stefan–Boltzmann constant, 5.64 × 10^{-8} W/m^{2}K^4
$Q_{IR,S,P}$ radiative heat transfer between the plant layer and the top substrate layer, W/m^2
$Q_{convection,plants}$ sensible heat flux between plants and surround air by convection, W/m^2
$Q_{convection,substrate,cov}$ sensible heat flux between substrate underneath plants and surround air by convection, W/m^2
Q_E soil evaporative flux, W/m^2
Q_{film} heat transfer from the substrate to the environment by means of evaporation (Q_T), convective heat transfer ($Q_{S,P}$), and radiative heat transfer (Q_{IR}), W/m^2
Q_{sun} incoming solar radiation, W/m^2 K
$Q_{s,s}$ sensible heat flux between green roof substrate and surround air by convection, W/m^2
$Q_{conduction}$ conductive heat flux through green roof substrate, W/m^2
h_{conv} convective heat transfer for plant layer, W/m^2 K
h_{sub} total convective heat transfer for green roof substrate covered by plants, W/m^2 K
h_{por} convective heat transfer for porous media (plants), W/m^2 K
LAI leaf area index [(leaf area)/(soil surface)]
ET evapotranspiration, or latent heat flux by convection, W/m^2
γ Psychrometric constant = $C_pP/0.622i_{fg}$
r_s stomatal resistance to mass transfer, s/m
r_a aerodynamic resistance to mass transfer, s/m
$e_{s,o}$ vapor pressure at the evaporative surface for the roofs with plants, kPa
e_{air} vapor pressure of the air, kPa
VWC(h) volumetric water content at pressure head h (cm), cm^3 cm^{-3}
θr, θs, θm residual and saturated water contents, fictitious(extrapolated) parameter, cm^3 cm^{-3}
α constant related to the inverse of the air-entry pressure, cm^{-1}
n, m n is measure of the pore-size distribution, $m = 1 - 1/n$
$q_{j,\theta}$ heat flux for time θ, W/m^2
Y_n, X_n CTF coefficient, W/m^2 K
$t_{j,\theta}$ surface temperature, C
φ_n dimensionless flux coefficient

moisture levels can change seasonally and diurnally, causing temporal variability for thermal conductivity and specific heat capacity. When a green roof substrate goes from dry to saturated conditions, thermal conductivity and specific heat capacity increase significantly. Therefore, it is necessary to understand substrate composition and moisture levels to be able to accurately simulate the green roof thermal performance as a component in the total building energy balance. Appropriate plant selection considers the environmental conditions specific to the climate zone. Growth success of green roof plants is expected to be partially dependent on the similarity between the roof eco-region and the plant's native habitat [9]. For example, *Sedum* are common plants used in extensive green roofs, but a study reported that some *Sedum* species could have poor performance in hot and humid areas because they are not well adept to these conditions [10].

Building location and selection of green roof components play important roles in green roof thermal performance. However, when estimating the thermal performance of green roofs, most previous studies considered only location or green roof components [11,12]. The current study investigated the effects of different plant species and substrates on thermal performance of green roof buildings located in different climate zones. Based on the simulations, this study recommends a few strategies for green roof component selection in several climates to improve the thermal performance of green roofs.

This study analyzed seven plant species and five substrates commonly used in green roofs. The study approach is divided in two steps: (1) conduct experiments to measure and analyze thermal properties of plants and substrates; and (2) simulate and analyze thermal performance of different green roofs using the measured properties.

2. Experimental approach

This investigation used seven plant species and five substrate types to evaluate the effects of different plants and substrates on the thermal performance of a green roof. Fig. 1 shows a photo of selected plant species and substrates. The plant species shown in Fig. 1 are: 1) *Sedum spurium* (*Dragon's Blood*), 2) *Sedum hispanicum*, 3) *Sedum rupestre Angelina*, 4) *Sedum sexangulare*, 5)*Sedum tomentosum*, 6) a tray with mixed *Sedum* species, and 7) *S. spurium*. The substrate materials are: 1) Norlite (Norlite expanded shale aggregate, Norlite LLC Cohoes, NY), 2) Perlite, 3) Expanded clay (Garick LLC, Cleveland OH), 4) "Cellar market" (a custom blended locally sourced roof media composed of sandstone aggregate and

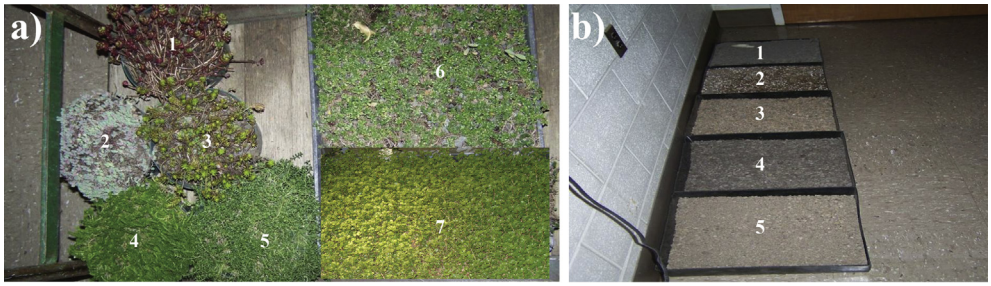

Fig. 1. Selected green roof materials: (a) plant species, (b) substrates.

Penn State compost), and 5) Rooflite media (Laurel Valley Soils, Avondale, PA).

This study also analyzed the relationship between substrate density and thermal properties so that future studies can calculate thermal properties from this relationship instead of performing a new set of measurements. Overall, the experimental measurements characterized different soils by their mineral phase composition, thermal conductivity, volumetric heat capacity and spectral reflectivity, while the plant materials were tested for their spectral reflectivity.

To get a general idea of the substrate components, the various substrates were first characterized by powder X-ray diffraction (XRD) to determine the mineral phases. X-ray diffraction (XRD) is a well-established method for phase identification of crystalline materials by comparing the XRD data with standard materials. The samples were analyzed using a Scintag diffractometer (Scintag, Inc., 707 Kifer Road, Sunnyvale, CA 94086) with CuKα X-rays, which are generated from a Cu tube in the XRD instrument and a germanium solid state detector. Its accuracy for diffraction data is within $\pm$0.5%. Diffraction patterns were collected with a step size of 0.020° 2θ and at the rate of 4° 2θ per minute. The X-ray counts at each step are saved to a file. X-ray counts of the diffracted beam are collected as a function of two theta (degrees) in a diffractometer.

The spectral reflectivity of substrate and plants was calculated from the spectral reflectivity measurements using a portable spectrometer. This study used a commercially available spectrometer (ASD FieldSpec4 Standard-Res portable spectroradiometer) with a range of 350–2500 nm. This device has the wavelength accuracy 0.5 nm, and the spectral resolution of 3 nm at 700 nm and 10 nm at 1400/2100 nm. The experimental setup used a calibrated lamp mounted on a tripod with the same spectral profile as the sun's spectrum to represent the light source. The data collection first used a calibrated white reference panel to calculate the reference reflectance factor. Furthermore, the substrate and plant samples were placed at the same relative position between the lamp and the target as the lamp and the reference panel. Each substrate and plant sample's reflectance factor was measured twice with a difference lower than the spectral resolution of the spectrometer.

The substrate thermal properties investigated in this study are thermal conductivity and volumetric heat capacity. The thermal conductivity is a key parameter in the conductive heat transfer process that defines the thermal loads on a building. The volumetric heat capacity signifies the heat storage potential of a substrate [13]. These thermal properties depend on mineral composition, dry density, water content and temperature [14]. The green roof substrate is a porous material, so the substrate sample measurements used a dual needle probe, which is a variation of transient line heat source method defined in IEEE 442-1981 [15] and ASTM D5334 [16] standards. A commercial transient heat flow probe (Decagon KD2 Pro) was used to determine thermal conductivity and volumetric heat capacity from a set of temperature measurements taken at 1 s intervals over a 30 s heating time and a 30 s cooling time. This probe had two 1.3 mm diameter $\times$ 30 mm length needles with 6 mm distance between each other. A line source heater provided a temperature increase measured at both probe locations as a function of time. The uncertainty of measuring thermal conductivity and volumetric heat capacity was within $\pm$10% [17]. Each substrate sample was slightly compacted into a metal can with the inner diameter of 8 cm and the height of 11 cm. Therefore, the distance from the edge of the can to the needles was larger than 1.5 cm in each direction, which is a requirement to preserve the measurement accuracy. The probe was inserted into the middle of the substrate samples and the reading started after 15 min to prevent errors caused by contact resistance between the probe and the substrate samples [17]. For each substrate type, the processes of sampling and measurement were repeated three times with 20 min interval between the measurements. In addition, the substrate density was measured by sampling the substrates' weight and volume with 3 replicate measurements.

3. Measured properties of different *Sedum* plants and substrates

The tested plant materials included different *Sedum* plant species as the most popular plant materials for extensive green roofs that do not require watering. The substrate materials included products from several different manufacturers as well as one custom blended material. The measured mineral components, spectral reflectivity, and thermal properties give an insight into properties of these popular green roof materials.

3.1. Mineral components of substrates

The substrates and their detailed mineral components, as determined by X-ray diffraction, are listed in Table 1. Figs. 2 and 3 show the XRD patterns of different substrates with peaks of various minerals identified. Norlite, Perlite, Expanded clay, "Cellar market", and Rooflite substrates absorbed 13%, 24%, 15%, 2%, and 25% water content by weight, respectively as measured by equilibrating the samples in water.

3.2. Spectral reflectivity measurements

Compared to regular roof assemblies, green roofs can reduce roof solar radiation absorption during the summer. The reflectivity of a material indicates the amount of reflected incident solar radiation. Figs. 4 and 5 show the spectral reflectivity of substrates and plant species, respectively, from 350 nm to 2500 nm wavelengths. The figures show that changes in spectral reflectivity with respect to wavelength are similar for different substrates and plant species.

Table 1
Names and components of substrates.

Substrate name	X-ray diffraction analyses; minerals in order of abundance
Norlite	Mainly quartz, SiO_2 (sand); trace feldspar; trace dolomite (Ca–Mg carbonate); trace leucite; No distinct clay peaks. This porous material is produced by vitrifying shale rock in a kiln.
Perlite	Mainly quartz, SiO_2 (sand); trace dolomite (Ca–Mg carbonate); trace feldspar; trace cristobalite, another type of SiO_2. This is heated volcanic glass material mixed with sand.
Expanded Clay	Mainly quartz, SiO_2 (sand); trace leucite; trace dolomite (Ca–Mg carbonate) No distinct clay peaks probably because of amorphization by heating.
"Cellar Market"	Mainly quartz, SiO_2 (sand); moderate dolomite (Ca–Mg carbonate); moderate kaolinite clay; slight mica clay and slight chlorite clay. This is the only sample that shows clays.
Rooflite media	Mainly quartz, SiO_2 (sand); trace leucite; trace dolomite (Ca–Mg carbonate) No distinct clay peaks.

However, the spectral reflectivity can vary for different types of substrates or plants at the same wavelength. The spectral reflectivity of substrates increases up to 0.15 when the wavelength changes from 350 to 950 nm. Among the tested substrate samples for wavelengths above 950 nm, "Cellar Market" has the highest spectral reflectivity of 0.17, while Norlite has the smallest value of 0.07. For tested plants, the spectral reflectivity increased and achieved the highest range when the wavelength ranged from 800 to 1000 nm. This is typical plant behavior as plants tend to absorb most incoming solar radiation in the photosynthetically active radiation (PAR) range from 400 to 700 nm; further increase of reflectivity of the radiation at longer wavelengths is not useful for photosynthetic purposes. In addition, there is a 0.3 difference in reflectivity in this range, but little difference outside of it, possibly because plants are more sensitive to visible light.

3.3. Thermal properties of substrates

The volumetric specific heat (mJ/(m^3 K)) is the heat required to raise the temperature of one cubic meter by 1 K, and is calculated as the product of specific heat (C_p) and density (ρ):

$$C = C_p \times \rho \tag{1}$$

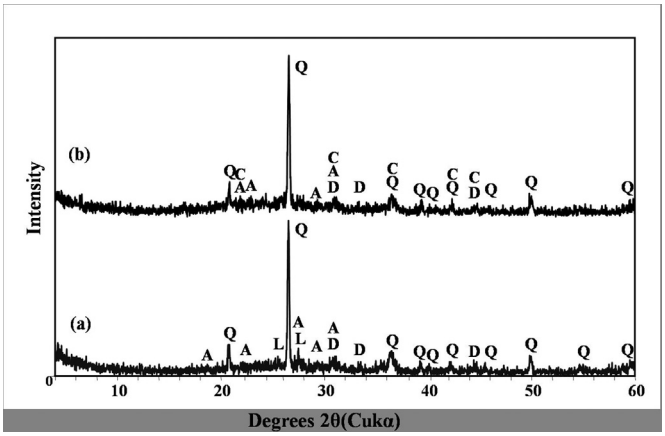

Fig. 2. X-ray diffraction patterns of (a) Norlite and (b) Perlite samples. Q = Quartz, D = Dolomite, A = Albite, C = Cristobalite, L = Leucite.

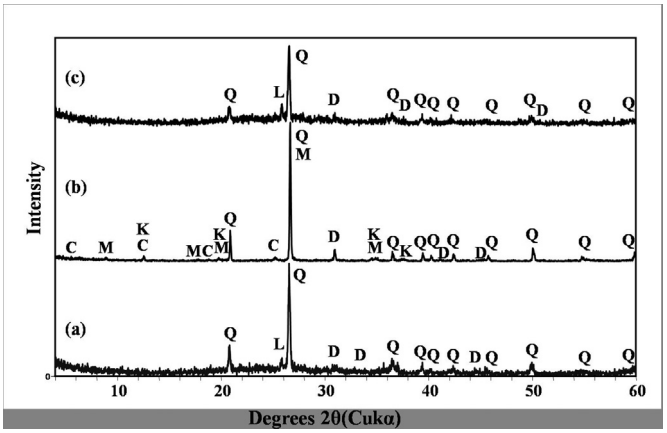

Fig. 3. X-ray diffraction patterns of (a) Expanded Clay, (b) "Cellar Market", and (c) Rooflite media: Q = Quartz, D = Dolomite, L = Leucite, M = Mica, C = Chlorite, K = Kaolinite.

Previous experiments have demonstrated a relationship between soil thermal conductivity (k) and soil density [18]. This study confirms that green roof substrates followed similar trend for both dry and saturated substrates as shown in Figs. 6 and 7. Fig. 6 shows the average results for all the substrates analyzed under dry and wet (saturated) conditions. In both cases, there is a strong linear correlation between density and thermal conductivity. Furthermore, Fig. 7 shows that a linear relationship also exists between the volumetric specific heat and density. Their respective linear equations are shown in Equations (2)–(5):

$$k(\text{wet}) = 0.0016\rho - 0.7485 \tag{2}$$

$$k(\text{dry}) = 0.0003\rho + 0.0405 \tag{3}$$

$$C(\text{wet}) = 2.6966 - 1172.1\frac{1}{\rho} \tag{4}$$

$$C(\text{dry}) = 1.8055 - 740.1\frac{1}{\rho} \tag{5}$$

To understand how identified differences in material properties affect the overall thermal performance of a green roof, this study used numerical simulations for the month of July as a representative summer month.

4. Numerical simulations using a validated green roof model

This study used a previously validated green roof model with the measured thermal properties of tested plants and substrate materials [19]. The green roof model simulated different green roof assemblies for the month of July in the Typical Meteorological Year (TMY3) [27], and for four cities representing different climate zones in the U.S. The green roof model considers heat and mass transfer processes between the sky, plants, and substrate, and the validation shows that the model predicts the heat and mass transfer accurately [5,19]. To account for water balance of the substrate, volume water content (VWC) was calculated by EnergyPlus [20] with precipitation data from TMY3 files.

4.1. Description of the green roof model

The green roof model was originally developed as a quasi-steady state heat and mass transfer green roof model [21,22], developed

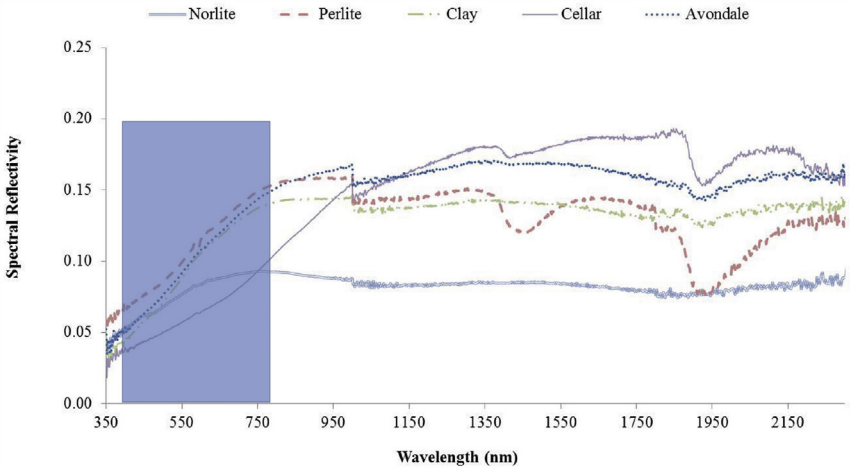

Fig. 4. Spectral reflectivity of five types of substrate.

from data collected in a "Cold Plate" apparatus set in an environment chamber [21]. Furthermore, this model was validated under outdoor environmental conditions using conduction transfer functions to account for the dynamic behavior of the green roof in an actual building [19]. This model covers all of the relevant heat and mass transfer phenomena as well as their interactions, and uses the simultaneous equation solver Engineering Equation Solver [23]. Fig. 8 shows the thermal circuit that incorporates the heat transfer phenomena considered in the model. Note that Fig. 8 was originally developed for steady state conditions [21], and later improved to model transient phenomena through the substrate using Conduction Transfer Functions (CTF) coefficients [22].

The green roof model simulates all chosen green roof assemblies based on a few assumptions: (1) the leaf area index (LAI) equal to 2.5, (2) the substrate thickness equal to 0.075 m, (3) the minimum stomatal resistance equal to 700 s/m, (4) an indoor air temperature of 20 °C so the model only considered the interaction between the green roof assembly and the outdoor environment, (5) plant extinction coefficients assumed to be 0.7–0.83, and (6) the plant coverage equal to 0.75. These values were based on previous work with the same plant species [20,21]. The assumption that all studied plant species have the same stomatal resistance and stomatal functions is a limitaion due to difficulties in measuring and/or obtaining data from the literature. For succulent plants, such as the studied *Sedum* plants, the stomatal resistance value is within a range of 450–1000 s/m, while for desert plants the stomatal resistance value is within a range of 225–1125 s/m [21]. The VWC for green roof substrates came from the precipitation data in TMY3 weather data files, calculated by EnergyPlus [20], and assuming no irrigation during the simulation time period.

4.1.1. Energy balance equations for a green roof

The energy balance equations for plant and substrate in the green roof model assumed negligible thermal storage and metabolic rates, so the absorbed short wave radiation by the plant and substrate can be expressed as:

$$R_{sh,abs,plants} = Q_{film,plants} + Q_{IR} \quad (6)$$

$$R_{sh,abs,substrate} = -Q_{IR} + Q_{s,p} + Q_{substrate} + Q_{IR,sky} + Q_E \quad (7)$$

Where $R_{sh,abs,plants}$ is the absorbed solar radiation by the plants, Q_{IR} is the radiative heat transfer between the plants and the top substrate layer; and $Q_{film,\ plants}$ represents the heat transfer between the plants and the surrounding environment by means of latent (transpiration) heat, convective and radiative heat transfer. In Equation (3), $R_{sh,abs,substrate}$ is the absorbed solar radiation by the substrate underneath the plants, Q_{IR} is the long wave radiation between the plant and the top substrate layer, Q_S is the convective

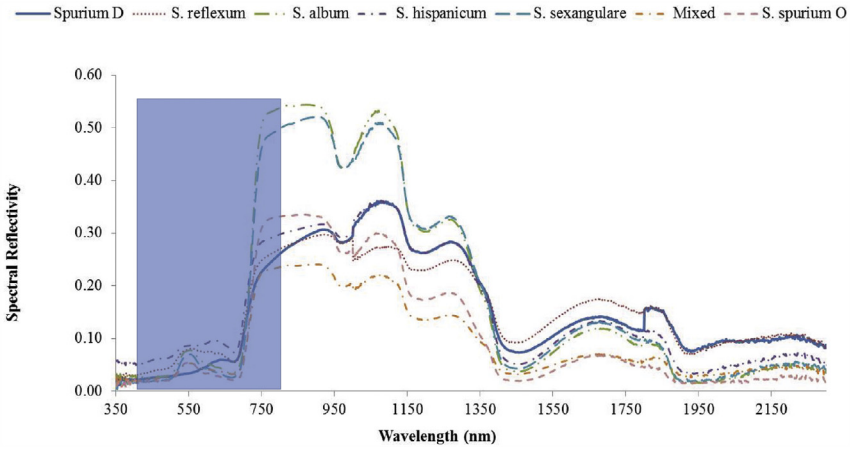

Fig. 5. Spectral reflectivity of seven plant species.

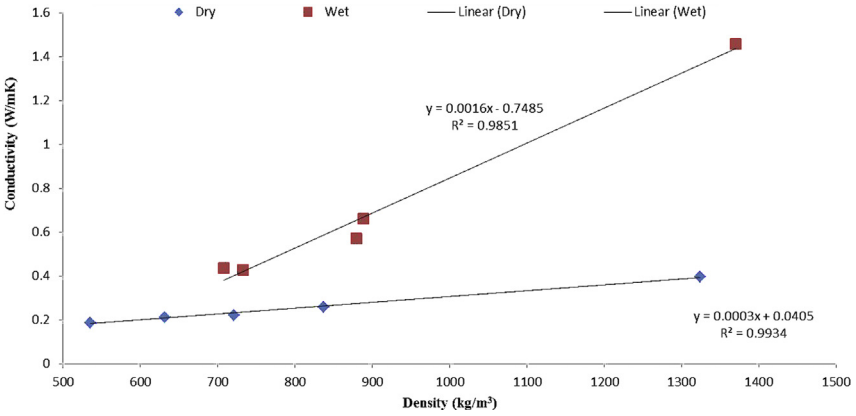

Fig. 6. Linear relationship between k and density for the tested substrates.

heat transfer between the top substrate layer and the surrounding air, $Q_{substrate}$ is the conductive heat fluxes through the green roof substrate, and $Q_{IR,sky}$ is the long wave radiation exchanged between the substrate and the sky.

4.1.2. Thermal radiation for green roof components

The thermal radiation between sky, plants, and green roof substrate can play an important role in green roof thermal performance, especially when the sky is clear and without clouds. The green roof model calculated thermal radiation from the following equations:

$$Q_{IR,plants,sky} = \left(1-\tau_{plants,IR}\right)\varepsilon_{plants}\sigma\left(T_{plants}^4 - T_{sky}^4\right) \quad (8)$$

$$Q_{IR,substrate,cov,sky} = \left(\tau_{plants,IR}\right)\varepsilon_{substrate}\sigma\left(T_{plants}^4 - T_{sky}^4\right) \quad (9)$$

The transmittance of thermal radiation ($\tau_{plants,IR} = e^{-kLAI}$), stands for radiation not intercepted by any leaf. $\tau_{plants,IR}$ was calculated by the same equation as $\tau_{plants,solar}$ with a different extinction coefficient. In Equations (8) and (9), ε_{plants} represents plant emissivity and $\varepsilon_{substrate}$ is the substrate emissivity, σ is Stefan–Boltzmann constant, 5.64×10^{-8} W/m^{2}K^4.

4.1.3. Long wave radiation between plant and substrate

Radiation exchanges between the plant layer and the top layer of substrate was difficult to simulate due to irregular surface geometries of the two involved media. To simplify the calculations, the two layers were assumed to be two infinite parallel plates/surfaces, since this added simplicity does not compromise the accuracy of the calculations:

$$Q_{IR,S,P} = \left(1-\tau_{plants,IR}\right)\frac{\sigma\left(T_{plants}^4 - T_{top,substrate}^4\right)}{\frac{1}{\varepsilon_{substrate}} + \frac{1}{\varepsilon_{plants}} - 1} \quad (10)$$

where τ_{IR} is the transmittance of radiation, T_{plants} and $T_{top,substrate}$ are plant temperature and temperature of top layer of substrate respectively.

4.1.4. Convective heat transfer

The convective heat transfer at the substrate was calculated using an equation developed for convection of porous media [24], assuming the air speed in the porous media is 1/3 of the air speed above the plants [25]:

$$Q_{convection,plants} = \beta LAI h_{conv}\left(T_{plants} - T_{air,ref}\right) \quad (11)$$

$$Q_{convection,substrate,cov} = h_{sub}\left(T_{substrate,top} - T_{air,ref}\right) \quad (12)$$

The substrate convective heat transfer coefficient ($h_{sub} = h_{por} \times h_{conv}/h_{por} + h_{conv}$) is based on the Nusselt number for porous media ($Nu_{por} = 1.128Pe^{0.5}$) [26], which comes from the Péclet number ($Pe = 0.3V_{air}Length/\alpha_{por}$) [24,25]. The constant coefficient β was set to 3 for vegetated sections of the green roof and 2.1 for the section of the roof without plants, based on previous research for convection heat on roofs [27].

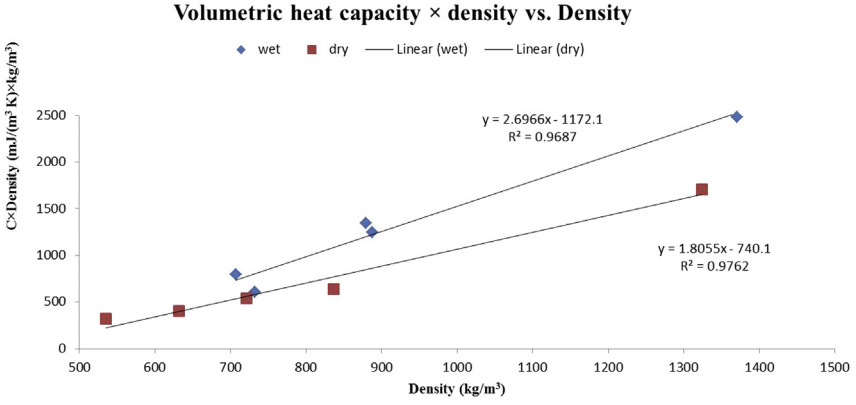

Fig. 7. Linear relationship between volumetric heat capacity and density for the tested substrates.

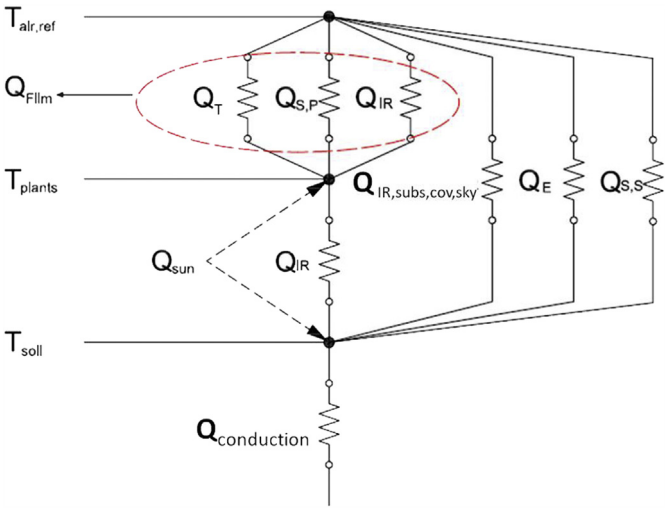

Fig. 8. Thermal circuit for heat fluxes considered in the green roof model.

4.1.5. Evapotranspiration

The substrate evaporation and plant transpiration were calculated using vapor pressure differential between the surrounding air and the evaporating surface shown by Equation (13) [21].

$$\mathrm{ET} = \mathrm{LAI}\frac{\rho C_p}{\gamma(r_s + r_a)}(e_{so} - e_{air}) \tag{13}$$

The plant transpiration depends on the plant stomatal resistance, the plant's resistance to water losses. In this model, the stomatal resistance is variable as it depends on environmental parameters such as the solar radiation, vapor pressure, temperature, and water content in the soil and plants. The soil evaporation also depends on the vapor pressure differential and the substrate water content. Additional details on the evapotranspiration model equations are available in the literature [21].

4.1.6. Conduction heat transfer

Following similar approach as in our previous validation study [22], the effect of the substrate thermal mass is calculated using Conduction Transfer Functions obtained from EnergyPlus. CTFs are widely used in building energy simulation programs because they relate the current conduction heat fluxes to current and past surface temperatures and heat fluxes using several coefficients that depend on the construction assembly properties and the simulation time step [28]. However, CTFs only allow the use of constant physical thermal properties, thus CTFs were obtained using average substrate thermal properties, including density, k, C_p, and C based on the following equation format:

$$q_{j,\theta} = -Y_0 t_{j,\theta} - \sum_{n=1}^{N_y} Y_n t_{j,\theta-n\delta} + X_0 t_{j,\theta} + \sum_{n=1}^{N_x} X_n t_{j,\theta-n\delta} + \sum_{n=1}^{N_q} \Phi_n q_{j,\theta-n\delta} \tag{14}$$

4.1.7. Volume water content (VWC)

The volume water content was calculated in EnergyPlus based on its internal green roof water balance model [29], which allows specified inputs including spectral reflectivity of plants and substrate thermal properties (density, conductivity, specific heat) and soil moisture conditions. The model has simplified moisture balance equations to account for precipitation, irrigation, and moisture transport between top and bottom substrate layers [20]. The calculation performs the advanced moisture diffusion calculation method, and the moisture transport model uses a finite difference method to divide the substrate into layers (nodes). The calculated substrate water content was then input into the green roof model to perform the heat balance. The VWC was calculated by the modified Mualem–van Genuchten model implemented in EnergyPlus [20,29]:

$$\mathrm{VWC(h)} = \begin{Bmatrix} \theta_r + \dfrac{\theta_m - \theta_r}{(1 + |\alpha h|^n)^m} & h < h_s \\ \theta_s & h \geq h_s \end{Bmatrix} \tag{15}$$

4.2. Green roof components

From top to bottom, the green roof assemblies consist of: (1) a plant layer which was assumed to have a height of 5 cm, (2) 7.5 cm substrate layer, (3) two layers of polypropylene fabric layers, (4) 2.5 cm of thick foam drainage/protection board made from chunks of recycled closed cell polystyrene, and (5) 0.2 cm PVC waterproof membrane layer. There were 35 possible combinations of green roof assemblies. Instead of simulating all the possible assemblies, this study chose only the plants and substrates with the highest and lowest reflectivity shown in Table 2, since the reflectivity directly affects absorbed radiation that contributes to cooling loads. Solar reflectivity was calculated using data shown in Figs. 4 and 5 and ASTM Standard G173-03 [5,30]. These plants were *S. tomentosum* and Mixed Species, and the substrates were Rooflite and Norlite. *S. tomentosum* and Rooflite media substrate were the base case to compare with the other green roof assemblies shown in Table 3.

Table 2
Reflectivity of the tested plants and substrates.

Green roof material	Name	Solar reflectivity
Plants	*Sedum tomentosum*	0.23
	Sedum sexangulare	0.22
	Sedum hispanicum	0.18
	Sedum rupestre Angelina	0.16
	Spurium delosperma	0.15
	Sedum spurium	0.14
	Mixed species	0.11
Substrates	Rooflite media	0.13
	Perlite	0.12
	Expanded Clay	0.12
	"Cellar Market"	0.11
	Norlite	0.08

Table 3
Three cases indicate simulated green roof assemblies.

Case	Plants	Substrates
1	*Sedum tomentosum*	Rooflite media
2	Mixed species	Rooflite media
3	*Sedum tomentosum*	Norlite

Table 4
Representative cities for the selected four U.S. climate zones.

City	Climate zone	Climate type
Austin, TX	2A	Hot
Sacramento, CA	3B	Warm
Nashville, TN	4A	Mixed
Chicago, IL	5A	Cool

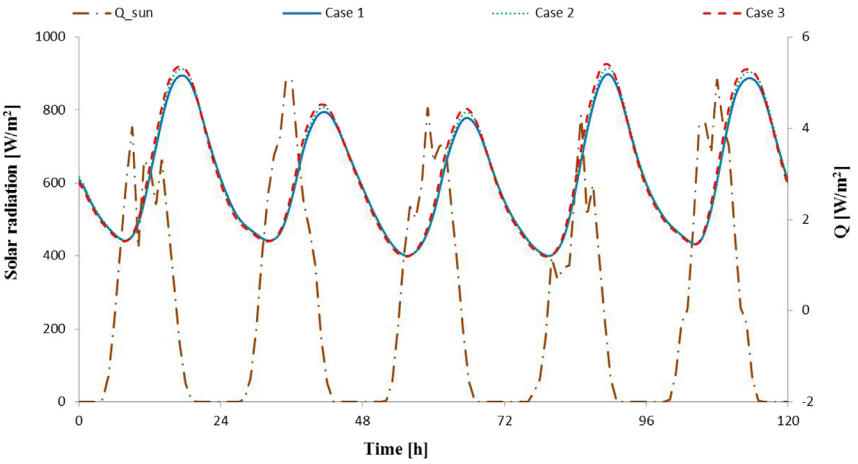

Fig. 9. Comparison of solar radiation and simulated substrate heat fluxes (Q) through green roof assemblies during five days of July in Austin, TX.

4.3. Locations and weather data inputs

The U.S. has seven climate zones, of which two zones (6 and 7) were omitted from this study because of small cooling loads during the July study period, and another zone (1) was omitted because it represents only a small percent of land area in the mainland U.S. Table 4 shows representative cities for the remaining four climate zones [31].

The design R-value for low slope insulated commercial roofs from ASHRAE Std. 90.1- 2004 is 2.8 m^2 °K/W for buildings located in climate zones 2 to 5. Typical Meteorological Year (TMY) 3 weather data files for each city were inputs in EES.

5. Simulation results and discussion

Three green roof assemblies in four locations yields twelve cases listed in Tables 3 and 4 Since the current study aims to evaluate thermal performance of green roofs during the summer, July was chosen as the representative month of summer for the simulations at 15-min intervals. The simulation results provided substrate heat fluxes and net radiation. Substrate heat fluxes indicate reduced heat transferred through substrates, while net radiation represented incident heat fluxes on the roof assemblies. This study presents green roof thermal performance over a 5-day period for a detailed investigation.

5.1. Heat fluxes through the green roof substrate

The substrate heat fluxes define the green roof's ability to reduce the cooling loads from the building enclosure. Fig. 9–12 compare the incoming solar radiation to the substrate heat fluxes of the three green roof assemblies listed in Table 3. In all four locations, the heat fluxes follow the changing incoming solar radiation with a time lag of approximately 6 h due to thermal storage. The heat fluxes through the green roof substrate are similar, with the flux variations for different assemblies ranging from 0.1 to 0.4 W/m^2as shown in Figs. 9 and 11. The results practically indicate no performance difference between substrates or plant species with respect to the cooling loads from the roof. The lack of the substrate flux sensitivity to the assembly variations is due to the insulation layer installed under the green roof assemblies, which had the thermal conductivity of 3 W/(m K). To illustrate the influence of the insulation layer, this study deployed the green roof model for the same green roof assemblies, but without insulation, using Chicago as the location. The simulations of uninsulated roof used Case 1 as the base case comparison, and the simulated results show that the average percentage of peak heat flux difference was 25% for Case 2

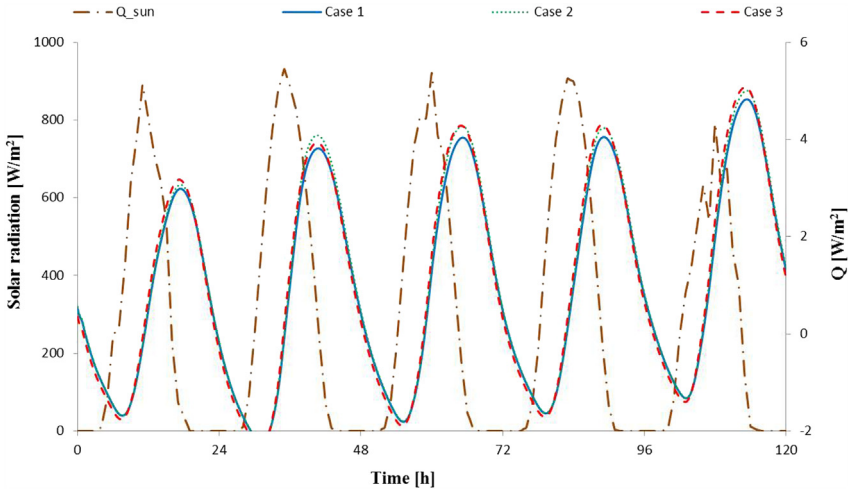

Fig. 10. Comparison of solar radiation and simulated heat fluxes (Q) through green roof assemblies during five days of July in Sacramento, CA.

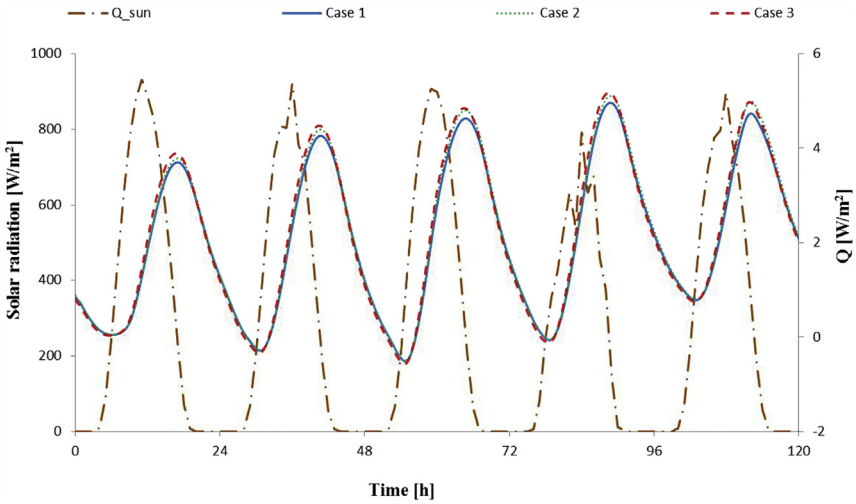

Fig. 11. Comparison of solar radiation and simulated heat fluxes (Q) through green roof assemblies during five days of July in Nashville, TN.

compared to Case 1, and 14% for Case 4 compared to Case 1. This difference between cases is significantly higher than that for the insulated roofs: -3% for Case 2 and 8% for Case 4 when compared to Case 1. The positive percentage values indicate a comparative increase, while the negative percentage values indicate a comparative decrease in the heat flux through the substrate.

5.2. Green roof net radiation

The net radiation combines the long-wave radiative heat fluxes and solar radiation absorbed by plants and substrates, and influences the temperature of green roof assemblies. The temperature of green roof assemblies can affect the building microclimate, conductive and convective heat transfer through the roof, and influence thermal load. Therefore, the net radiation is an important component of the thermal circuit of green roof model to be analyzed. Fig. 13–20 show the simulated net radiation for the four selected cities. For each city, the first figure shows solar radiation compared to simulated net radiation for each case, and the second figure has a finer resolution that shows the net radiation differences between Case 1 and the other two cases. These figures show that the net radiation pattern is following the incoming solar radiation pattern in most cases. The absorbed net radiation increases and reaches its peak during the morning; then decreases with the solar radiation in the afternoon. The green roof assemblies then release radiation to the surrounding environment during the night at a rate of 60–70 W/m^2. For all locations, the plant species had an overwhelming effect on the net radiation, while the substrate type had limited effects. This can be seen from Figs. 14, 16, 18 and 20 showing that the net radiation difference between Case 4 and Case 1 was nearly 0 W/m^2 during the simulation time period. The net radiation difference between different cases, representing different roof assemblies, reaches peak during the daytime and disappears during the night. Plant species with lower reflectivity, such as mixed *Sedum* used in Case 2, results in a larger value of the net radiation compared to the net radiation of *S. tomentosum* used in Case 1.

Table 5 shows the absolute and percentage difference between Case 1 and Case 2 of all-data average and peak-only average heat flux values for net radiation, convection and latent heat transfer. Case 1 and Case 2 have the same substrate type and thus the same R-value, so plant species in the green roof assembly caused the difference in heat flux values. The peak difference in net radiation from plant species is around 16%. Convective heat loss difference was responsible for a part of the difference in the peak net

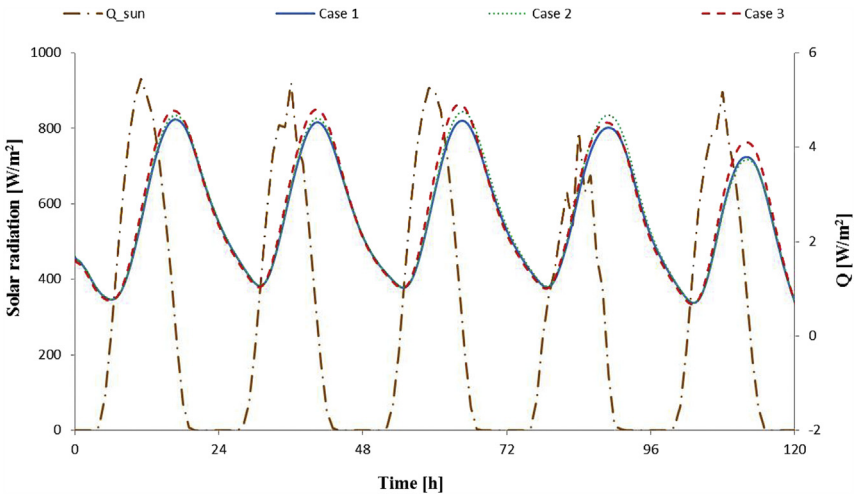

Fig. 12. Comparison of solar radiation and simulated heat fluxes (Q) through green roof assemblies during five days of July in Chicago, IL.

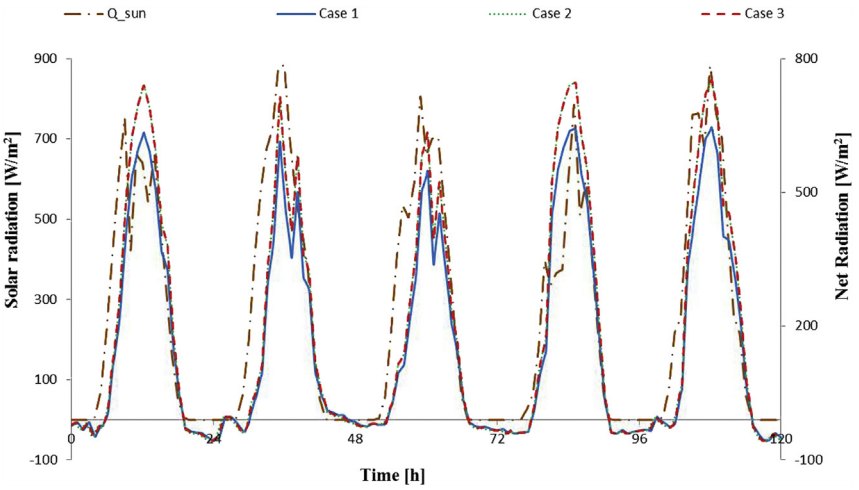

Fig. 13. Comparison of solar radiation and simulated net radiation during five days of July in Austin, TX.

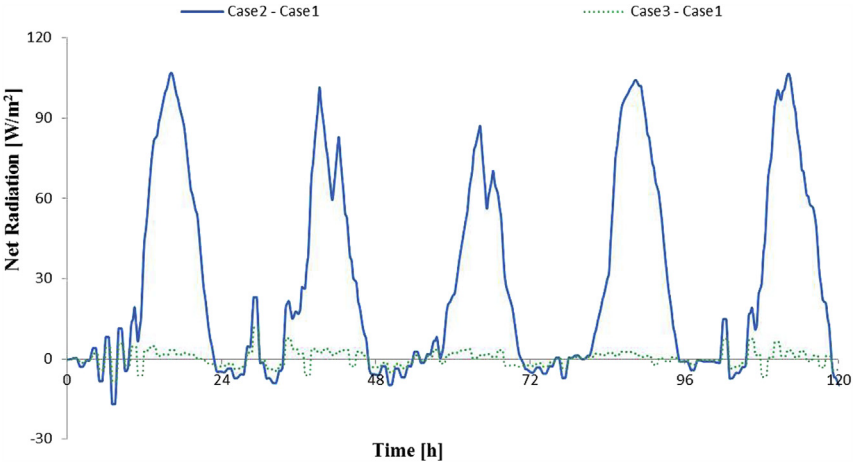

Fig. 14. Comparison of simulated net radiation difference between cases during five days of July in Austin, TX.

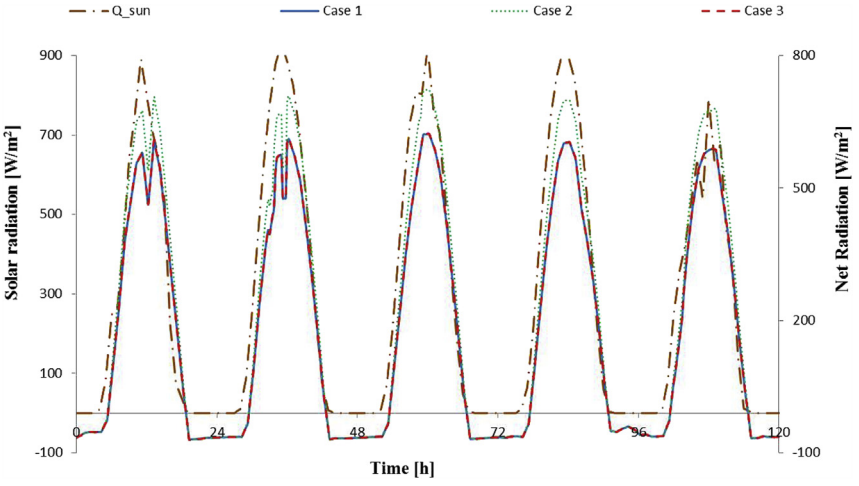

Fig. 15. Comparison of solar radiation and simulated net radiation during five days of July in Sacramento, CA.

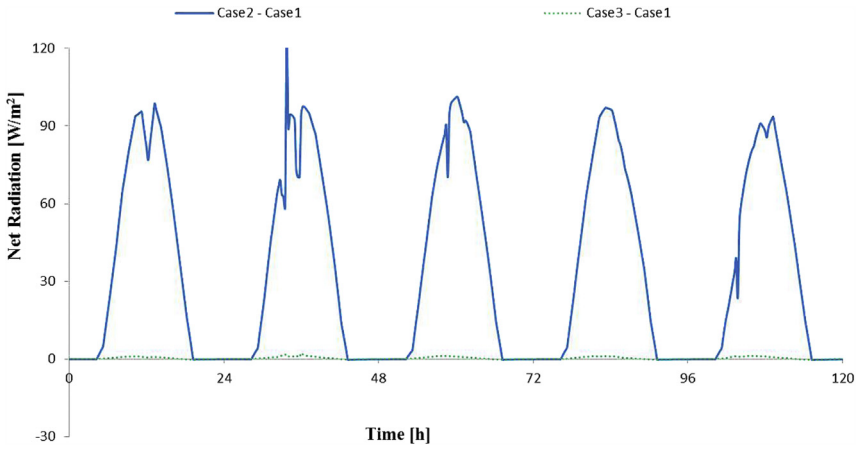

Fig. 16. Comparison of simulated net radiation difference between cases during five days of July in Sacramento, CA.

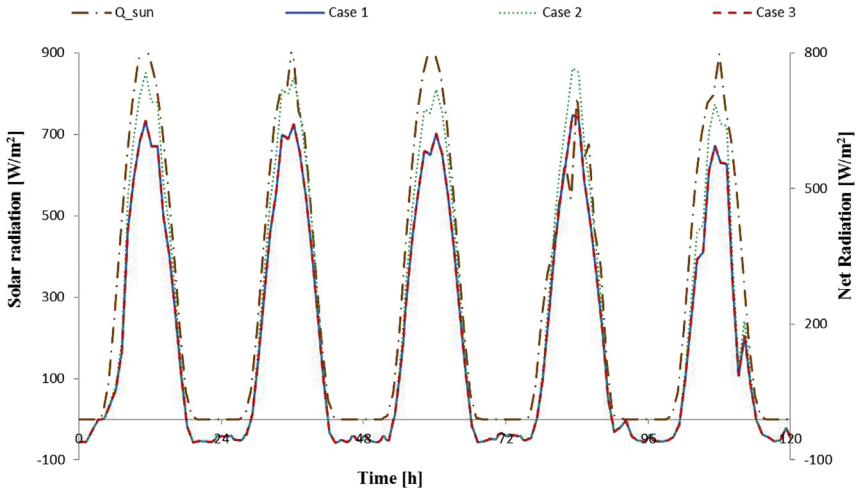

Fig. 17. Comparison of solar radiation and simulated net radiation during five days of July in Nashville, TN.

radiation, with the latent heat transfer differences accounting for the rest. The differences in simulated peak latent heat transfer were small (less than 5%) because the green roof model assumed the same stomatal resistance for different plant species. In field conditions, the differences between Case 1 and Case 2 should be larger because the stomatal resistance is different.

Among the four locations, Chicago had the largest net radiation differences for both peak average (16%) and all-data average (20%), which indicates importance of green roof materials for the thermal performance of green roofs located in Chicago. Plant species result in relatively smaller difference in the net radiation for buildings located in Austin and Sacramento, probably because these cities

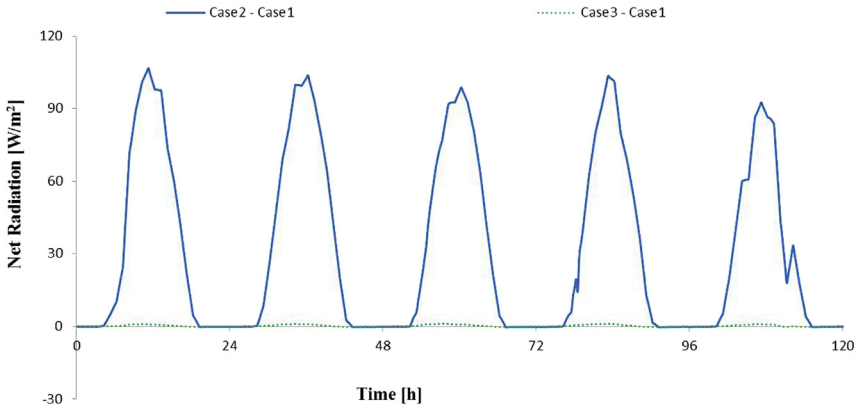

Fig. 18. Comparison of simulated net radiation difference between cases during five days of July in Nashville, TN.

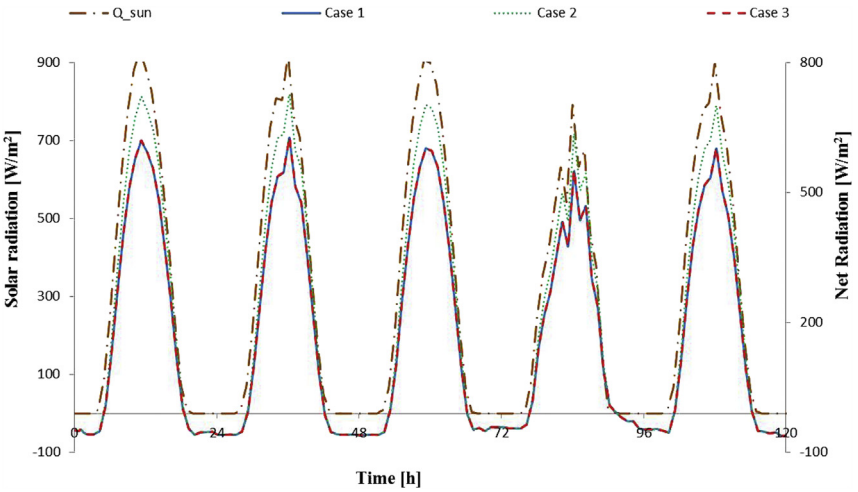

Fig. 19. Comparison of solar radiation and simulated net radiation during five days of July in Chicago, IL.

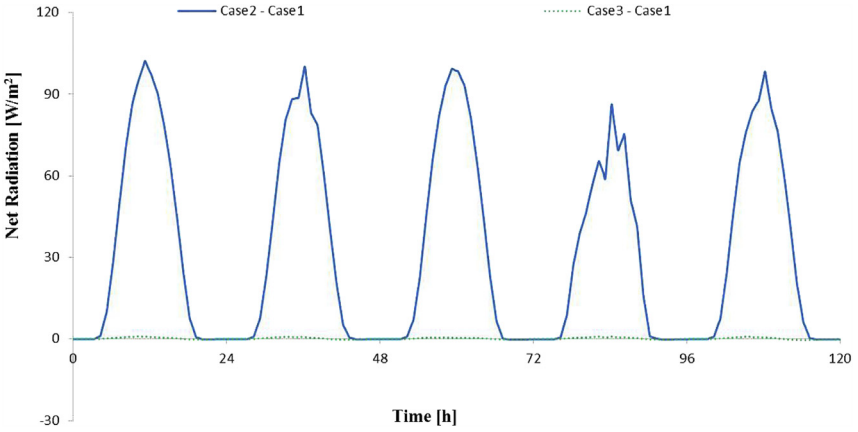

Fig. 20. Comparison of simulated net radiation difference between cases during five days of July in Chicago, IL.

have hot and humid summers that *Sedum* species do not tolerate well [11].

6. Conclusions

From the thermal point of view, plants and substrates are the two most important components in the green roof design. By simulating the thermal performance of different green roof assemblies, this study examined how different types of plants and substrates affect the green roof thermal performance in four different climate zones. The investigation measured thermal properties for seven plant species and five substrates types, then three combinations of plants and substrates were selected for simulation using a previously developed and validated green roof model. The substrate heat fluxes and the net radiation were chosen to represent the green roof thermal performance. Several conclusions follow from the simulation results:

1) Both substrate heat fluxes and net radiation varied with the trends in solar radiation, while the substrate heat fluxes had a time lag of approximately 6 h due to the substrate thermal mass.
2) The insulation installed under the green roof assemblies plays an important role in the thermal performance of green roofs. The insulation diminished the differences in substrate heat fluxes for different green roof assemblies, and therefore, limited the influence of substrates and plant species selection. In addition, the spectral reflectivity of plant species had a strong effect on the net radiation, while the thermal properties of various substrate types did not cause a significant difference because of the high LAI and plant coverage.
3) Plant spectral reflectivity has a significant effect on the net radiation. Plants with a lower reflectivity, such as the mixed *Sedum* plants in Case 2, resulted in larger values of the net radiation. The difference in net radiation between cases peaked at 16% during the day, and was eliminated at night. Therefore,

Table 5
Comparison between Case 1 and Case 2 for different locations.

Type	Differences	Austin	Sacramento	Nashville	Chicago
Peak data average for the analyzed 5 days	Net radiation Difference W/m^2, (%)	97.3, (16.2)	96.5, (15.9)	101.1, (16.0)	100.8, (16.3)
	Convective Difference W/m^2, (%)	90.3, (34.1)	97.8, (36.8)	96.7, (33.3)	103.7, (38.6)
	Latent Difference W/m^2, (%)	9.86, (2.79)	0.56, (0.12)	<0.001, (0.026)	6.34, (1.74)
All data average	Net radiation Difference W/m^2, (%)	26.9, (17.9)	33.0, (19.7)	30.9, (19.5)	31.3, (20.2)

based on the assumptions made in this study, compared to other plant species for the climate zones considered, *S. tomentosum* is the preferred choice to minimize cooling load.

4) Green roof assemblies have different thermal performance in different climate zones. Plant species showed an average difference of 16% in the peak net radiation and 20% in the average net radiation for Chicago. The green roof assemblies located in Nashville showed a 20% average difference in the net radiation, indicating that the thermal properties of plants should be considered in the plant selection process for better green roof thermal performance. However, the thermal performance of green roof assemblies in climate zone 2 and 3, represented by Austin and Sacramento, were not dependent on the green roof material selection due to the hot and humid summers that *Sedum* species do not tolerate well.
5) Readers should consider that this study compares only the spectral properties of the studied *Sedum* plants because the assumed stomatal resistance function was the same for all plants.

References

[1] Czemiel Berndtsson J. Green roof performance towards management of runoff water quantity and quality: a review. Ecol Eng 2010;36:351–60.
[2] Sailor DJ, Elley TB, Gibson M. Exploring the building energy impacts of green roof design decisions-a modeling study of buildings in four distinct climates. J Build Phys 2012;35:372–91.
[3] Zhao M, Srebric J. Assessment of green roof performance for sustainable buildings under winter weather conditions. J Central South Univ Technol Engl Ed 2012;19:639–44.
[4] Liu KKY. Sustainable building envelope – garden roof system performance; 2004. Presented at the 2004 RCI Building Envelope Symposium, New Orleans, Louisiana.
[5] IEEE. ASTM G173-03 standard tables for reference solar spectral irradiances: direct normal and hemispherical on 37° tilted surface. In: Proceedings of the IEEE standards committee. New York: Institute of Electrical and Electronics Engineers Inc.; 2008.
[6] Sailor DJ, Hutchinson D, Bokovoy L. Thermal property measurements for ecoroof soils common in the western U.S. Energy Build 2008;40:1246–51.
[7] Hiraiwa Y, Kasubuchi T. Temperature dependence of thermal conductivity of soil over a wide range of temperature (5–75 °C). Eur J Soil Sci 2000;51:211–8.
[8] Cengel YA. Heat transfer, a practical approach. New York: McGraw-Hill Higher Education; 2003.
[9] Dvorak B, Volder A. Green roof vegetation for North American ecoregions: a literature review. Landsc Urban Plan 2010;96:197–213.
[10] Livingston EH, Miller C, Lohr M. Green roof design and implementation in Florida; 2004. Presented at the The Second Annual Greening Rooftops for Sustainable Communities Conference.
[11] Niachou A, Papakonstantinou K, Santamouris M, Tsangrassoulis A, Mihalakakou G. Analysis of the green roof thermal properties and investigation of its energy performance. Energy Build 2001;33:719–29.
[12] Kotsiris G, Androutsopoulos A, Polychroni E, Nektarios PA. Dynamic U-value estimation and energy simulation for green roofs. Energy Build 2012;45:240–9.
[13] Kluitenberg GJ, Ham JM, Brislow KL. Error analysis of the heat pulse method for measuring soil volumetric heat capacity. Soil Sci Soc Am J 1993;57:1444–51.
[14] Dong Z, Chen-hui L, Long-shan X, and Jia-min M. "Experimental study on the thermophysical parameters of Cohesive soil by the transient method". In: *E-Product E-Service and E-Entertainment (ICEEE), 2010 International Conference on, 2010*. p. 1–4.
[15] IEEE. IEEE 442 guide for soil thermal resistivity measurements. In: Proceedings of the IEEE standards committee. New York: Institute of Electrical and Electronics Engineers Inc.; 1981.
[16] ASTM. Standard test method for determination of thermal conductivity of soil and soft rock by thermal needle probe procedure. Philadelphia: American Society for Testing and Materials; 2000.
[17] Decagon. KD2 pro specifications; 2006.
[18] Farouki OT. Thermal properties of soils. Clausthal-Zellerfeld, Germany: Trans Tech Publications; 1986.
[19] Tabares-Velasco PC, Zhao M, Peterson N, Srebric J, Berghage R. Validation of predictive heat and mass transfer green roof model with extensive green roof field data. Ecol Eng 2012;47:165–73.
[20] U. S. Department of Energy. EnergyPlus; 2013. V-8.0 ed.
[21] Tabares-Velasco PC, Srebric J. Experimental quantification of heat and mass transfer process through vegetated roof samples in a new laboratory setup. Int J Heat Mass Transf 2011a;54:5149–62.
[22] Tabares-Velasco PC, Srebric J. Predictive green roof model for assessment of heat transfer through a roof assembly in summer weather conditions. Build Environ 2012;49:310–23.
[23] F-Chart Software. Engineering equation solver; 2013.
[24] Bejan A. Convection heat transfer. 3rd ed. Hoboken, New Jersey: John Wiley and Sons; 2004.
[25] Deardorff JW. Efficient prediction of ground surface temperature and moisture, with inclusion of a layer of vegetation. J Geophys Res 1978;83:1889–903.
[26] Schuepp PH. Tansley review No. 59 leaf boundary layer. New Phytol 1993;125:477–507.
[27] Clear RD, Gartland L, Winkelmann FC. An empirical correlation for the outside convective air-film coefficient for horizontal roofs. Energy Build 2003;35:797–811.
[28] National Renewable Energy Laboratory. Typical Meteorological Year 3 [Online].
[29] Schaap MG, van Genuchten MT. A modified Mualem–van genuchten formulation for improved description of the hydraulic conductivity near saturation. Vadose Zone J 2006;5:27–34. /1 2006.
[30] Duffie JA, Beckman WA. Solar engineering of thermal processes. 3 ed. Wiley; 2006.
[31] ASHRAE. ASHRAE standard 90.1. Atlanta, GA: American Society of Heating, Refrigerating and Air-Conditioning Engineers, Inc.; 2007.